GEOCHRONOLOGICAL APPLICATIONS

As discussed in Chapter 1, geomagnetic secular variation exhibits periodicities between 1 yr and 10^5 yr. We learn in this chapter that geomagnetic polarity intervals have a range of durations from 10^4 to 10^8 yr. In the next chapter, we shall see that apparent polar wander paths represent motions of lithospheric plates over time scales extending to $>10^9$ yr. As viewed from a particular location, the time intervals of magnetic field changes thus range from decades to billions of years. Accordingly, the time scales of potential geochronologic applications of paleomagnetism range from detailed dating within the Quaternary to rough estimations of magnetization ages of Precambrian rocks.

Geomagnetic field directional changes due to secular variation have been successfully used to date Quaternary deposits and archeological artifacts. Because the patterns of secular variation are specific to subcontinental regions, these Quaternary geochronologic applications require the initial determination of the secular variation pattern in the region of interest (e.g., Figure 1.8). Once this regional pattern of swings in declination and inclination has been established and calibrated in absolute age, patterns from other Quaternary deposits can be matched to the calibrated pattern to date those deposits. This method has been developed and applied in western Europe, North America, and Australia. The books by Thompson and Oldfield (1986) and Creer et al. (1983) present detailed developments. Accordingly, this topic will not be developed here.

This chapter will concentrate on the most broadly applied of geochronologic applications of paleomagnetism: *magnetic polarity stratigraphy*. This technique has been applied to stratigraphic correlation and geochronologic calibration of rock sequences ranging in age from Pleistocene to Precambrian. Magnetic polarity stratigraphy (or *magnetostratigraphy*) has developed into a major subdiscipline within paleomagnetism and has drawn together stratigraphers and paleontologists working with paleomagnetists to solve a wide variety of geochronologic problems.

To understand the principles of magnetic polarity stratigraphy, it is necessary to understand the development of *geomagnetic polarity time scales*. The first portion of this chapter presents the techniques that are used to develop the geomagnetic polarity time scale (GPTS) and gives examples of the resulting time scales. This discussion necessarily involves the presentation of some classic examples of magnetic polarity stratigraphy; magnetostratigraphy has both required the development of geomagnetic polarity time scales and contributed to that development. In the second half of this chapter, we discuss case histories of applications of magnetic polarity stratigraphy to geochronologic problems. This approach is used because the principles and strategies of magnetostratigraphy are best understood in the context of particular geochronological applications. Topics such as sampling and data analysis and quality are developed as they arise in presentation of the case histories.

DEVELOPMENT OF THE GEOMAGNETIC POLARITY TIME SCALE

The discussion of the development of the geomagnetic polarity time scale presented here is necessarily brief and might not present the details that some readers desire. Detailed accounts of the development of the Pliocene–Pleistocene GPTS are given by Cox (1973) and by McDougall (1979). An excellent and

detailed review of the development of the polarity time scale is given by Hailwood (1989). For a history-of-science approach to the development of the GPTS and its critical role in the evolution of plate tectonic theory, the reader is referred to Glen (1982).

The Pliocene–Pleistocene

Modern development of the geomagnetic polarity time scale was initiated in the 1960s following advances allowing accurate potassium-argon (K-Ar) dating of Pliocene–Pleistocene igneous rocks. In general, igneous rocks with the same age but from widely separated collecting localities were found to have the same polarity. Age and magnetic polarity determinations of increasing numbers of igneous rocks were compiled and led to the development of the first geomagnetic polarity time scales in the 0- to 5-Ma time interval (Figure 9.1).

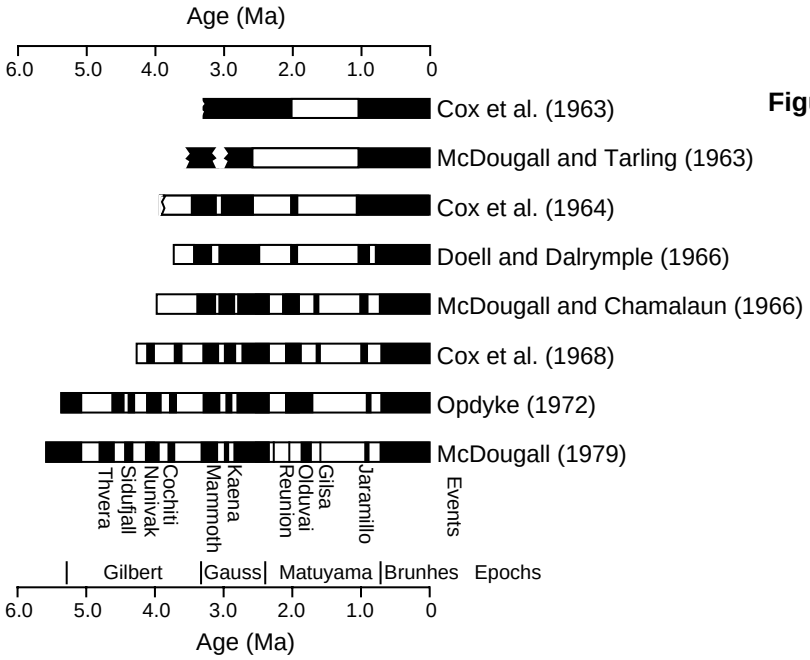

Figure 9.1 Evolution of the Pliocene–Pleistocene geomagnetic polarity time scale between 1963 and 1979. On this and all subsequent polarity columns or time scales, black intervals indicate normal polarity and white intervals indicate reversed polarity; references are given at the right of each time scale; the "event" and "epoch" nomenclature applied to this portion of the time scale is given at the bottom. Adapted from McDougall (1979).

When few age and polarity determinations were available, polarity intervals were thought to have durations of about 1 m.y. These polarity intervals were called *polarity epochs* and were named after prominent figures in the history of geomagnetism. But it soon became clear that shorter intervals of opposite polarity occurred within the polarity epochs. These shorter intervals were called *polarity events* and were named after the locality at which they were first sampled. We now understand that no fundamental distinction exists between polarity epochs and polarity events; polarity intervals of a wide spectrum of durations are possible. The polarity epoch and event nomenclature is basically an accident of history but is retained as a matter of convenience for this portion of the time scale.

During this early development, there were arguments as to whether the reversed-polarity igneous rocks were due to reversed polarity of the geomagnetic field or due to *self-reversal of thermoremanent magnetism*. Nagata et al. (1952) found an igneous rock (the Haruna dacite) that acquired a TRM antiparallel to the magnetic field in which it was cooled. This observation raised the possibility that all reversed-polarity igneous rocks had undergone self-reversal of TRM. The self-reversing TRM of the Haruna dacite was found to be carried by titanohematite of composition $x \approx 0.5$ (remember Chapter 2?). It turns out that self-reversal is a rare occurrence, accounting for perhaps 1% of reversed-polarity igneous rocks; intermediate composition titanohematites are rarely the dominant ferromagnetic minerals in igneous rocks. The internal consistency in geomagnetic polarity time scales derived from igneous rocks distributed worldwide verified that geomagnetic field reversals were the correct explanation for all but a few reversed-polarity igneous rocks.

A Pliocene-Pleistocene geomagnetic polarity time scale based primarily on K-Ar dating and paleomagnetic polarity determinations on igneous rocks is given in Figure 9.2. Some 354 age and polarity determinations were used to construct this time scale. Several important features of geomagnetic polarity history can be appreciated from this figure:

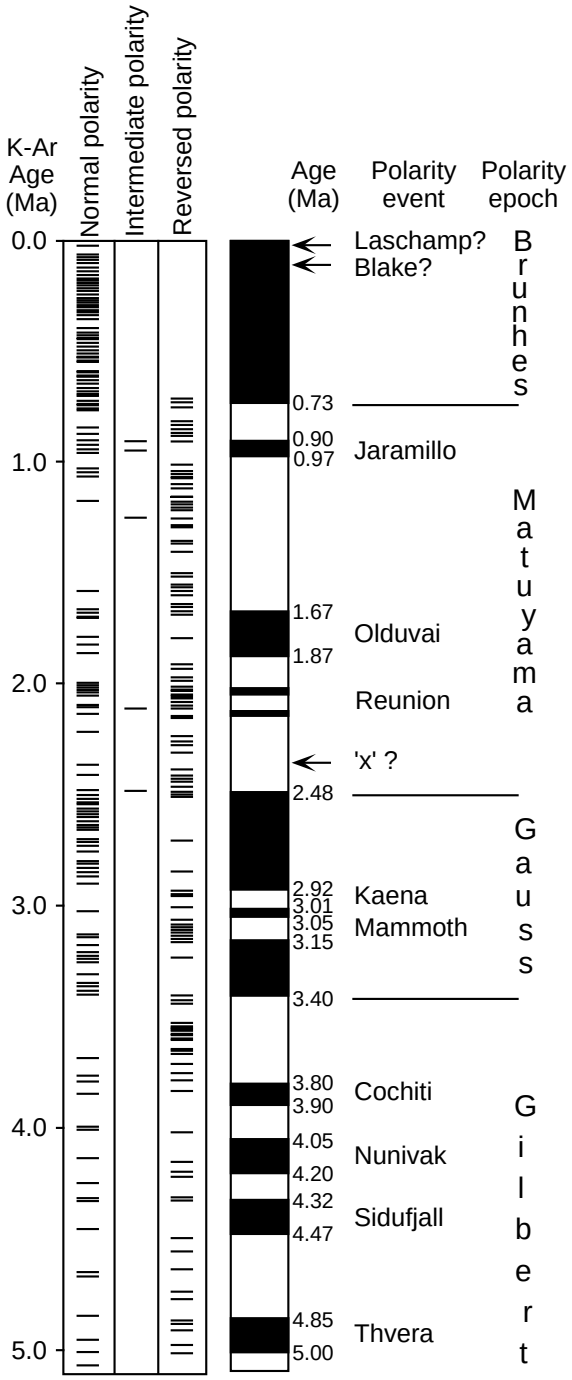

Figure 9.2 Pliocene-Pleistocene geomagnetic polarity time scale of Mankinen and Dalrymple (1979). Each horizontal line in the columns labeled normal polarity, intermediate polarity, or reversed polarity represents an igneous rock for which both K-Ar age and paleomagnetic polarity have been determined; auxiliary information from marine magnetic anomaly profiles and deep-sea core paleomagnetism has also been used to determine the polarity time scale; arrows indicate disputed short polarity intervals or geomagnetic "excursions"; numbers to the right of the polarity column indicate interpreted ages of polarity boundaries. Redrawn from Mankinen and Dalrymple (1979) with permission from the American Geophysical Union.

1. During the past 5 m.y., the <u>average</u> duration of polarity intervals is ~0.25 m.y. But there is a wide range of durations with the shorter duration intervals being more common.
2. Only about 1.5% of the observations are classified as "intermediate polarity." These intermediate-polarity rocks were probably magnetized while the geomagnetic field was in *polarity transition* between normal and reversed polarities. Polarity transition occurs quickly (probably within about 5000

years), and geomagnetic polarity reversals can be regarded as rapid, globally synchronous events. This feature of polarity reversals is central to many geochronologic applications of polarity stratigraphy.

3. Geomagnetic polarity reversals are randomly spaced in geologic time; they are the antithesis of square-wave or sine-wave behavior, so switches of polarity are not predictable. This means that patterns of four or five successive polarity intervals do not generally recur. Instead, the patterns of long and short intervals can be used as "fingerprints" of particular intervals of geologic time. This type of pattern recognition is essential to most geochronologic applications of polarity stratigraphy.

4. Analytical uncertainties that are inherent in radiometric dating generally limit application of this "dating and polarity determination" technique to the past 5 m.y. At an absolute age of 5 Ma, the typical error in radiometric age determination approaches the typical duration of polarity intervals. With the possible exception of detailed analysis of polarity stratigraphy in thick sequences of volcanic rocks such as in Iceland (McDougall, 1979), other techniques are required to decipher the GPTS for times older than 5 Ma.

Extension into the Miocene

Paleomagnetism of deep-sea cores provided important information about the geomagnetic polarity sequence prior to 5 Ma. An example polarity record in a deep-sea piston core is given in Figure 9.3. Provided that sediment accumulation took place without significant breaks, the DRM of a deep-sea core can allow accurate determination of the magnetic polarity sequence. Paleontological dating of sedimentary horizons is required to determine geologic ages, and correlation to a radiometrically dated polarity sequence is required to estimate absolute ages within individual deep-sea cores. In practice, numbers of deep-sea cores providing high-fidelity paleomagnetic records and paleontologic calibrations of the polarity sequence were required for determination of the geomagnetic polarity time scale. Example time scales determined by this method are those of Opdyke et al. (1974) and Theyer and Hammond (1974).

Marine magnetic anomalies

Marine magnetic anomaly profiles constitute the richest source of information about the sequence of geomagnetic polarity intervals from mid-Mesozoic to the present. The essentials of the seafloor spreading hypothesis (Vine and Matthews, 1963; Morley and Larochelle, 1964) explaining the origin of marine magnetic anomalies are presented in Figure 9.4. This hypothesis became a cornerstone of plate tectonic theory.

During seafloor spreading, upper mantle material upwells at a spreading ridge and solidifies onto the trailing edges of the oceanic lithospheric plates that are separating at the ridge. The oceanic crust forms the upper portion of this lithosphere and is composed of mafic igneous rocks including basaltic pillow lavas and feeder dikes. These basaltic rocks contain titanomagnetite and acquire a TRM during cooling in the geomagnetic field. The oceanic crust thus can be viewed as a limited-fidelity tape recording of past polarities of the geomagnetic field. But the polarity record in the oceanic crust is not determined by direct sampling.

The alternating polarities of TRM in the oceanic crust are depicted by the black (normal-polarity) and white (reversed-polarity) crustal blocks in Figure 9.4. These blocks of alternating TRM polarity generate *magnetic anomalies*. At mid to high latitudes, a normal-polarity block generates a magnetic field that adds to the regional geomagnetic field, resulting in a positive magnetic anomaly; the local magnetic field above the normal-polarity block is 100 to 1000 gammas (1 gamma = 10^{-5} Oe) higher than the regional value. For a reversed-polarity block, the resulting magnetic anomaly above the block is negative. By towing a magnetometer behind an oceanographic vessel and observing the magnetic field anomaly profile at the sea surface (the marine magnetic anomaly profile), it is possible to remotely sense the polarity of magnetization in the underlying oceanic crust. From the ridge crest outward to progressively older oceanic crust, observed marine magnetic anomaly profiles allow determination of the polarity of progressively older oceanic crust. The sequence of past geomagnetic polarities thus can be inferred from marine magnetic anomaly profiles.

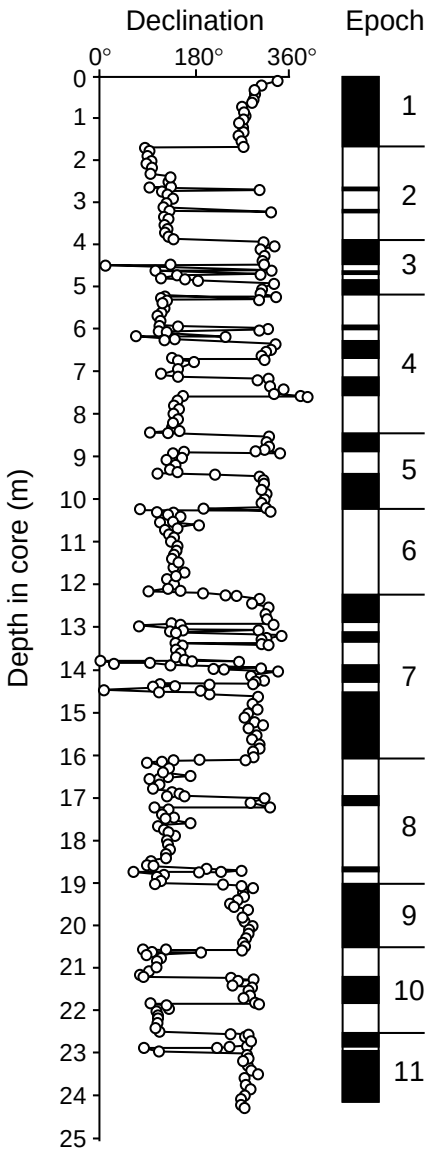

Figure 9.3 Change in paleomagnetic declination with depth in deep-sea piston core RC12-65 collected from the equatorial Pacific Ocean. The absolute declination is arbitrary because the core was not azimuthally oriented (declination at the top of the core was set to 360°); the oldest sediment at the base of the core is early Late Miocene (about 10 Ma absolute age); the interpreted magnetic polarity time scale was divided according to the "magnetic epoch" numbering system, which is now obsolete. Redrawn from Opdyke et al. (1974).

To estimate ages of past polarity intervals determined in this fashion, the rate of seafloor spreading must be determined. Because the Pliocene–Pleistocene GPTS is known independently (e.g., Figure 9.2), the pattern of normal-polarity and reversed-polarity blocks near the ridge crest is also known. This pattern must be linearly scaled according to the rate of seafloor spreading. A *model profile* is computed for an assumed rate of seafloor spreading and is compared with the observed magnetic anomaly profile. The rate of seafloor spreading is determined by matching the model and observed profiles as shown in Figure 9.4.

The first geomagnetic polarity time scale to use marine magnetic anomalies as its primary data base was that of Heirtzler et al. (1968). This GPTS is reproduced in Figure 9.5. Heirtzler et al. used observed magnetic anomaly profiles to infer a block model of the magnetic polarity of the oceanic crust in the South Atlantic. They determined the rate of spreading of the South Atlantic Ridge by matching the observed and model profiles using the independently known GPTS back to 3.35 Ma (the Gauss/Gilbert boundary). Using various marine geophysical evidences, Heirtzler et al. argued that the rate of seafloor spreading of the South Atlantic Ridge had been constant for the past 80 m.y. The age of oceanic crust in the South Atlantic and the age of inferred geomagnetic polarity intervals thus could be predicted. This procedure led to the polarity time scale of Figure 9.5, which must be considered one of the boldest and most accurate extrapolations in the history of Earth science. The subsequent 20 years of research has shown that this time scale was off by only about 5 m.y. at a predicted age of 70 Ma!

Two important features of the Heirtzler et al. (1968) GPTS are easily noticed: (1) During the Cenozoic, the total time in normal-polarity and reversed-polarity states was approximately equal; there was no significant *polarity bias* during the Cenozoic. (2) The rate of reversal of the geomagnetic field increased during the Cenozoic. In the Paleocene and Eocene, the average rate of polarity reversal was about 1/m.y., whereas the rate for the past 5 m.y. was about 4/m.y. Statistical analysis of geomagnetic polarity reversals and reversal rate changes has become a major subject in geomagnetism (see the review by Lowrie, 1989).

About nomenclature

A brief discussion about nomenclature applied to magnetic polarity intervals is required. We noted during dis-

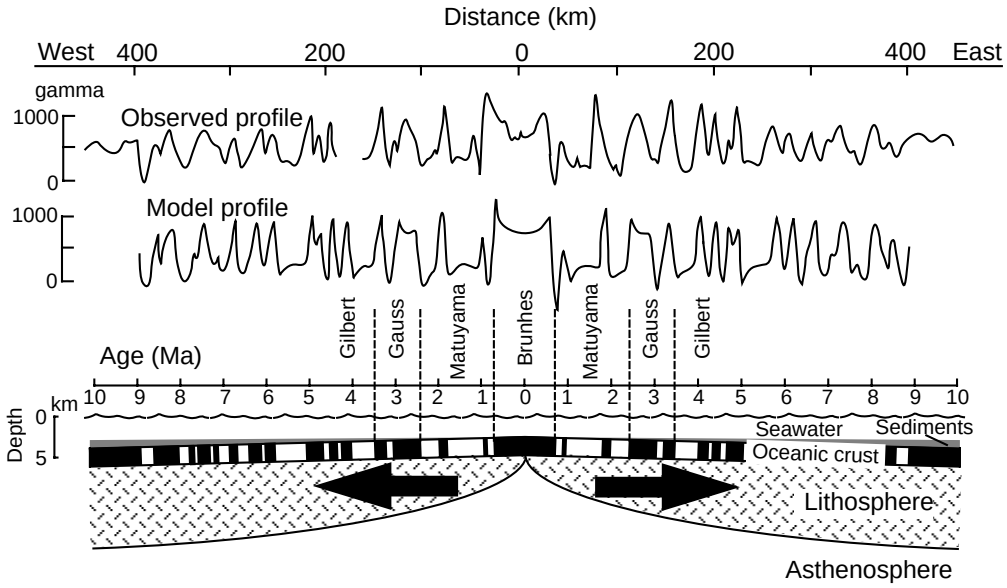

Figure 9.4 Formation of marine magnetic anomalies at an oceanic ridge undergoing seafloor spreading. The oceanic crust is the upper portion of the oceanic lithosphere forming at the ridge crest and being covered by an increasing thickness of oceanic sediments; the black (white) blocks of oceanic crust represent the normal (reversed) polarity TRM acquired during original cooling of the oceanic crust; blocks of crust formed during Pliocene-Pleistocene polarity epochs are labeled, and epoch boundaries are shown by dashed lines; the absolute age of oceanic crust is shown by the horizontal scale; the model profile is the computed sea-level magnetic anomaly profile produced by the block model of TRM polarity in the oceanic crust; the observed profile is the actual observed sea-level magnetic anomaly profile across the Pacific-Antarctic Ridge; the distance scale is given at the top of the figure; model and observed profiles are best matched by a half-spreading rate of 45 km/m.y. Adapted from Pitman and Heirtzler (1966), *Science*, v. 154, 1164–71, ©1966 by the American Association for the Advancement of Science.

cussion of the Pliocene–Pleistocene GPTS that a nomenclature system of polarity epochs and events was developed for this portion of the time scale. This system has been superseded for earlier portions of the time scale but is retained for the Pliocene–Pleistocene because of historical precedent.

The polarity epoch system was extended into the Miocene and Oligocene to describe polarity intervals found in deep-sea cores, but these earlier epochs were denoted by numbers. For example, in Figure 9.3, the Gilbert polarity epoch is designated Epoch 4, the preceding polarity epoch is designated Epoch 5, etc. But use of “epoch” to denote geomagnetic polarity intervals was in conflict with prior usage of “epoch” for a particular subdivision of geologic time.

When marine magnetic anomaly profiles were used to develop geomagnetic polarity time scales, an additional nomenclature problem became apparent. The prominent marine magnetic anomalies had been given numbers increasing away from spreading oceanic ridge crests. These *magnetic anomaly numbers* are noted on the Heirtzler et al. time scale in Figure 9.5. But what nomenclature should be applied to the normal-polarity time interval when the oceanic crust generating magnetic anomaly number 5 was produced? We can’t call it “epoch 5” because that name has already been applied to the polarity epoch preceding the Gilbert epoch. Some new system (not in conflict with previous geological nomenclatures) was required.

A system of geomagnetic *polarity chrons* was developed. Time intervals of geomagnetic polarity are now referred to by a chron designation that is tied to the marine magnetic anomaly numbering system. The normal-polarity time interval discussed in the previous paragraph is referred to as “polarity chron 5” (Cox, 1982). Reversed-polarity time intervals are referred to by using a suffix “r” to denote the reversed-polarity interval preceding a particular normal-polarity chron. For example, the reversed-polarity chron preceding

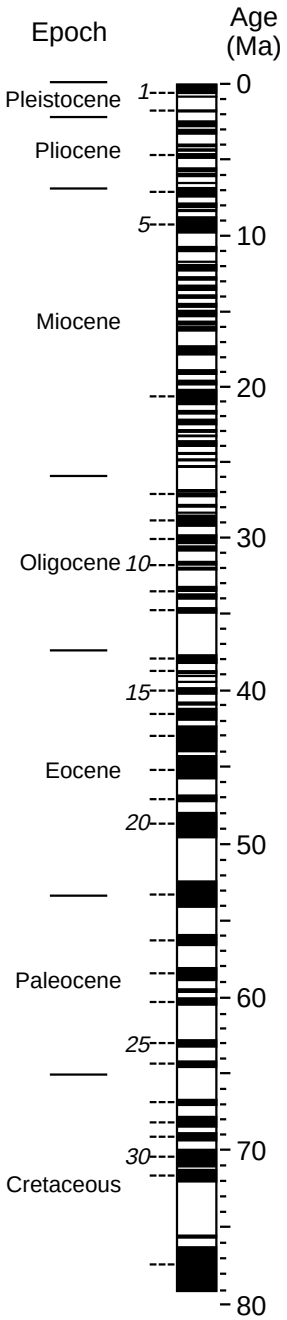

Figure 9.5 The geomagnetic polarity time scale of Heirtzler et al. (1968) determined from analysis of marine magnetic anomalies. Geologic epochs within the Cenozoic are shown at left; the numbers in italics at the left of polarity time scale are magnetic anomaly numbers; the predicted absolute age is given by the scale at the right of polarity column. Redrawn from Heirtzler et al. (1968) with permission from the American Geophysical Union.

chron 25 is designated chron 25r. This nomenclature system takes a little getting used to, but it does work. If you're not burned out by this discussion of nomenclature, detailed accounts are presented by Cox (1982) and Hailwood (1989).

Biostratigraphic calibrations

When the Heirtzler et al. (1968) GPTS was developed, ages of polarity chrons in the Paleogene were predicted by the assumed constant seafloor spreading rate of the South Atlantic Ridge. Testing the predicted ages of these polarity chrons was a major objective of the Deep Sea Drilling Project (DSDP). As shown schematically in Figure 9.4, marine sediments accumulate on newly generated oceanic crust. The age of the oldest sediment thus approximates the age of the oceanic crust.

Hundreds of DSDP cores (and cores drilled during the successor Ocean Drilling Program (ODP)) have been drilled in ocean basins over the past 25 years. To test the prediction of the Heirtzler et al. time scale that magnetic polarity chron 25 is Early Paleocene in age, a core could be drilled through the sediment to igneous basement at a site where marine magnetic anomaly 25 had been identified. Microfossils from that core could be identified by a paleontologist to allow determination of the geologic age of the oldest sediment. In fact the oldest sediment in DSDP cores drilled into oceanic basement formed during chron 25 have been found to be Late Paleocene rather than Early Paleocene in age. In this fashion, definitive sediment ages from numerous DSDP cores have required adjustments to the Heirtzler et al. (1968) polarity time scale. Additional mapping of marine magnetic anomalies has also resulted in some adjustments to the magnetic anomaly pattern itself. Particularly notable examples of geomagnetic polarity time scales developed in this way are those of LaBrecque et al. (1977) and Ness et al. (1980).

Paleontological dating of DSDP sediment cores provided "spot checks" on the polarity time scale. Magnetostratigraphic investigations of marine sedimentary sequences also have provided detailed biostratigraphic calibrations. The most important of these investigations (perhaps the most spectacular of all magnetostratigraphic studies) was that of the Late Mesozoic and Cenozoic pelagic limestone sequences in the Umbrian Apennines of Italy. (It is interesting to note that this paleomagnetic research was initiated by Walter Alvarez and Bill Lowrie to investigate the tectonic devel-

opment of the Appenines. Beyond the important magnetostratigraphic data obtained, subsequent research led to the discovery of iridium-enriched sediment at the Cretaceous/Tertiary boundary and advancement of the impact hypothesis for mass extinctions at this boundary (Alvarez et al., 1980).)

The paleomagnetic data obtained from the pelagic limestone sequence at Gubbio, Italy, are shown in Figure 9.6. Lowrie and Alvarez (1977) analyzed paleomagnetic samples collected at close stratigraphic spacings. The ChRM direction for each sample (corrected for tectonic effects) was used to compute the

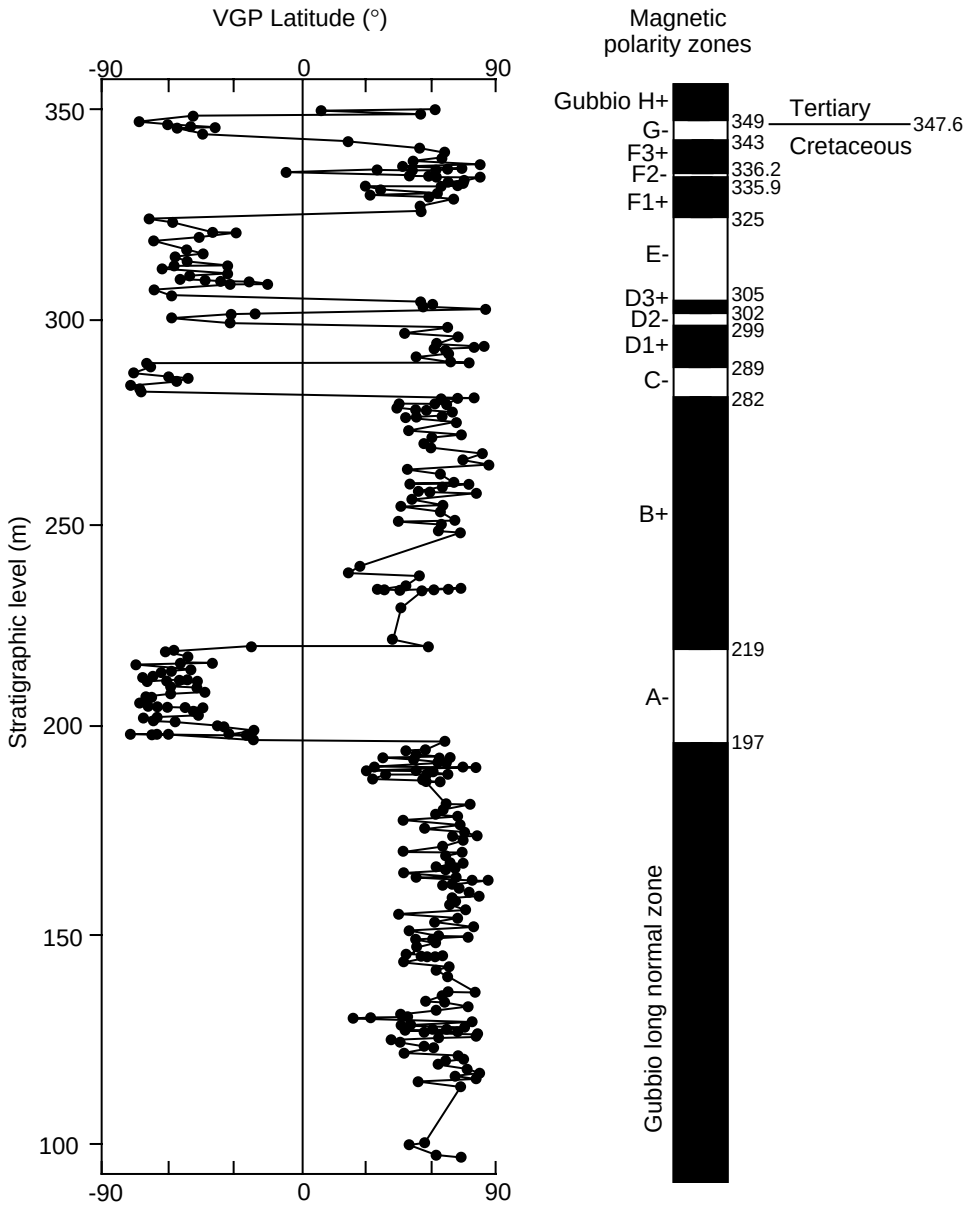

Figure 9.6 Magnetostratigraphic results from the Upper Cretaceous portion of the Scaglia Rossa section in the Umbrian Apennines near Gubbio, Italy. The virtual geomagnetic pole (VGP) latitude determined from the ChRM direction from each paleomagnetic sample is plotted against the stratigraphic level; the sequence of interpreted polarity zones is shown by the polarity column with stratigraphic levels of polarity boundaries (in meters) noted on the right side of the column; polarity zones are designated by the alphabetical system on the left side of column; the position of the Cretaceous/Tertiary boundary is noted at the right. Redrawn from Lowrie and Alvarez (1977) with permission from the Geological Society of America.

virtual geomagnetic pole (VGP) latitude for each stratigraphic horizon. Because VGP latitude is computed from both inclination and declination of ChRM, it is a convenient parameter for displaying results of a magnetostratigraphy investigation. A positive VGP latitude indicates normal polarity of the geomagnetic field at the time of ChRM acquisition, while a negative VGP latitude indicates reversed polarity.

The VGP latitudes from the Gubbio section (Figure 9.6) allow determination of *magnetic polarity zones* in the stratigraphic succession, the term "zone" being used to refer to a particular rock stratigraphic interval. These polarity zones are shown in Figure 9.6 and are labeled by using an alphabetical system. This is now common (and well-advised) practice in magnetostratigraphy. The observed paleomagnetic data (ChRM inclination, declination, VGP latitude, or some combination thereof) are plotted against stratigraphic position. These data are then used to define a *magnetic polarity zonation* for the stratigraphic section. For example, the stratigraphic interval between 219 and 282 m of the Gubbio section has positive VGP latitudes defining normal-polarity zone "Gubbio B+." The suffix "+" is used to denote normal-polarity zones, while "–" is used for reversed-polarity zones. In the Gubbio section, the Cretaceous/Tertiary boundary occurs within magnetic polarity zone Gubbio G– at the 347.6-m stratigraphic level.

A major contribution from the magnetostratigraphic research at Gubbio was the determination that the Cretaceous/Tertiary boundary occurs within magnetic polarity chron 29r. This determination was reached through the analysis presented in Figure 9.7. Here the magnetic polarity zonation from the Gubbio section is compared with the polarity pattern inferred from analysis of marine magnetic anomaly profiles in three different oceans. Although minor variability exists, the polarity patterns determined from the marine magnetic anomaly profiles can be unambiguously correlated to the Gubbio magnetic polarity zonation. For example, magnetic polarity zone Gubbio D1+ correlates with the normal-polarity interval associated with

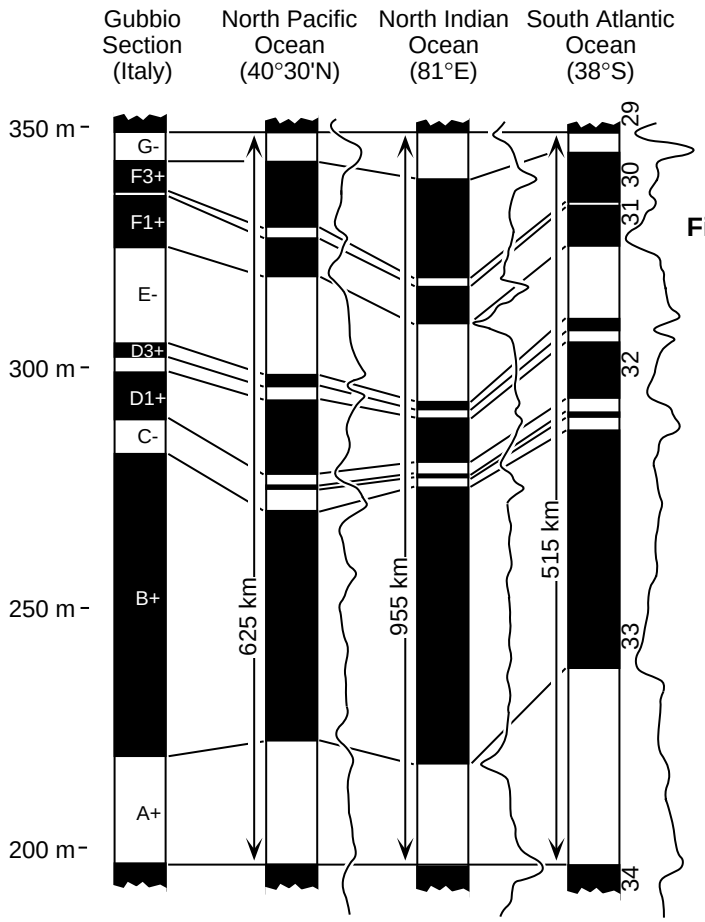

Figure 9.7 Correlation of magnetic polarity zones at the Gubbio section with polarity sequences interpreted from analyses of marine magnetic anomaly profiles in three oceanic areas. Magnetic anomaly numbers and magnetic profiles are shown to the right of each interpreted polarity sequence; linear scales of magnetic profiles are shown to the left of polarity sequences; polarity sequences are scaled so that the polarity boundaries at the beginning and end of the sequence are connected by horizontal lines. Redrawn from Lowrie and Alvarez (1977) with permission from the Geological Society of America.

magnetic anomaly 32. From this correlation, it is evident that the Cretaceous/Tertiary boundary (within polarity zone Gubbio G–) occurred during magnetic polarity chron 29r. Note that the Heirtzler et al. (1968) time scale (Figure 9.5) had predicted that the Cretaceous/Tertiary boundary occurred during chron 26r.

Paleomagnetic analyses of numerous stratigraphic sections in the Umbrian Appenines have allowed additional biostratigraphic calibrations of the GPTS (Figure 9.8). The biostratigraphic zonations of these stratigraphic sections have been determined in great detail, so the stratigraphic position of various geologic time boundaries are well known. The placement of geologic time boundaries within the pattern of polarity intervals thus can be determined. For example, the Paleocene/Eocene boundary occurs within a reversed-polarity zone correlative with magnetic polarity chron 24r.

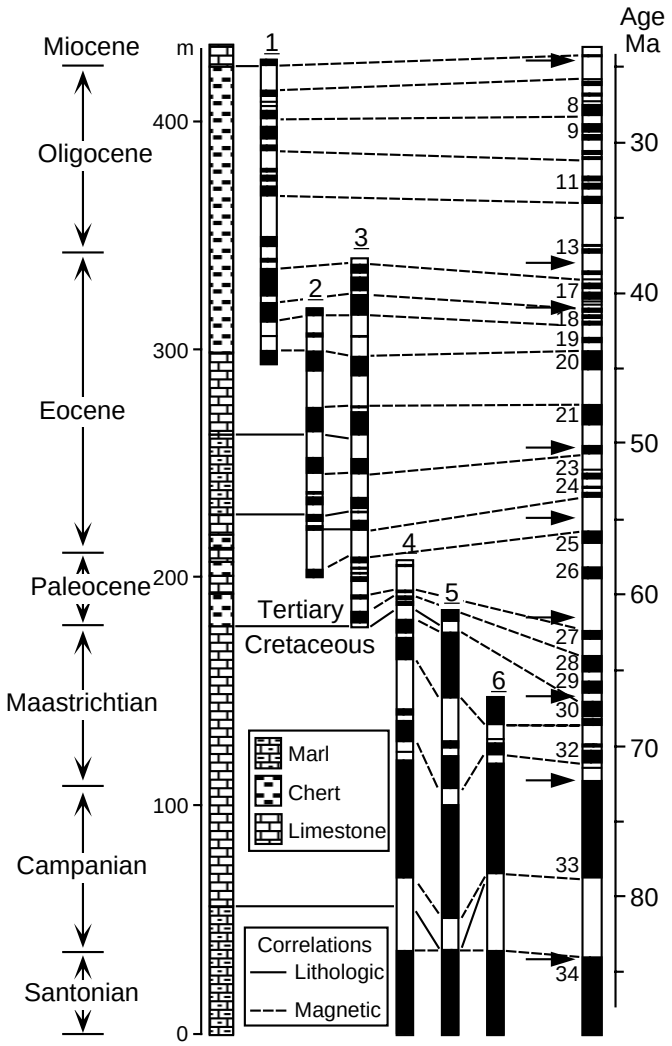

Figure 9.8 Correlations of Late Cretaceous through Cenozoic magnetostratigraphic sections in the Umbrian Apennines with the marine magnetic anomaly sequence. Age from foraminiferal zonation is shown at left; the dominant lithology is noted on the stratigraphic column (scaled in meters); polarity zones in individual columns are correlated with each other and with the marine magnetic anomaly sequence shown by polarity column at the right (magnetic anomaly numbers and paleontological calibration points (shown by the arrows) are noted at the left side of this column); the section numbers noted at the top of the columns are as follows: 1 Contessa quarry; 2 Contessa road; 3 Contessa highway; 4 Bottaccione; 5 Moria; 6 Furlo upper road. Adapted from Lowrie and Alvarez (1981) with permission from the Geological Society of America.

A Late Cretaceous–Cenozoic GPTS

The results from DSDP cores and magnetostratigraphic investigations can allow biostratigraphic calibration of the geomagnetic polarity time scale. But what about absolute age calibration? Development of geologic time scales involves association of isotopically dated horizons with the biostratigraphic zones. There are numerous geologic time scales because evaluating these absolute age calibrations is complex. The process of developing a geomagnetic polarity time scale invariably requires the choice of a geologic time scale. A Late Cretaceous-Cenozoic GPTS developed as part of a larger geological time scale project (and influenced by an effort to minimize changes in seafloor spreading rates) is given in Figure 9.9. This is the time scale of Cox (1982).

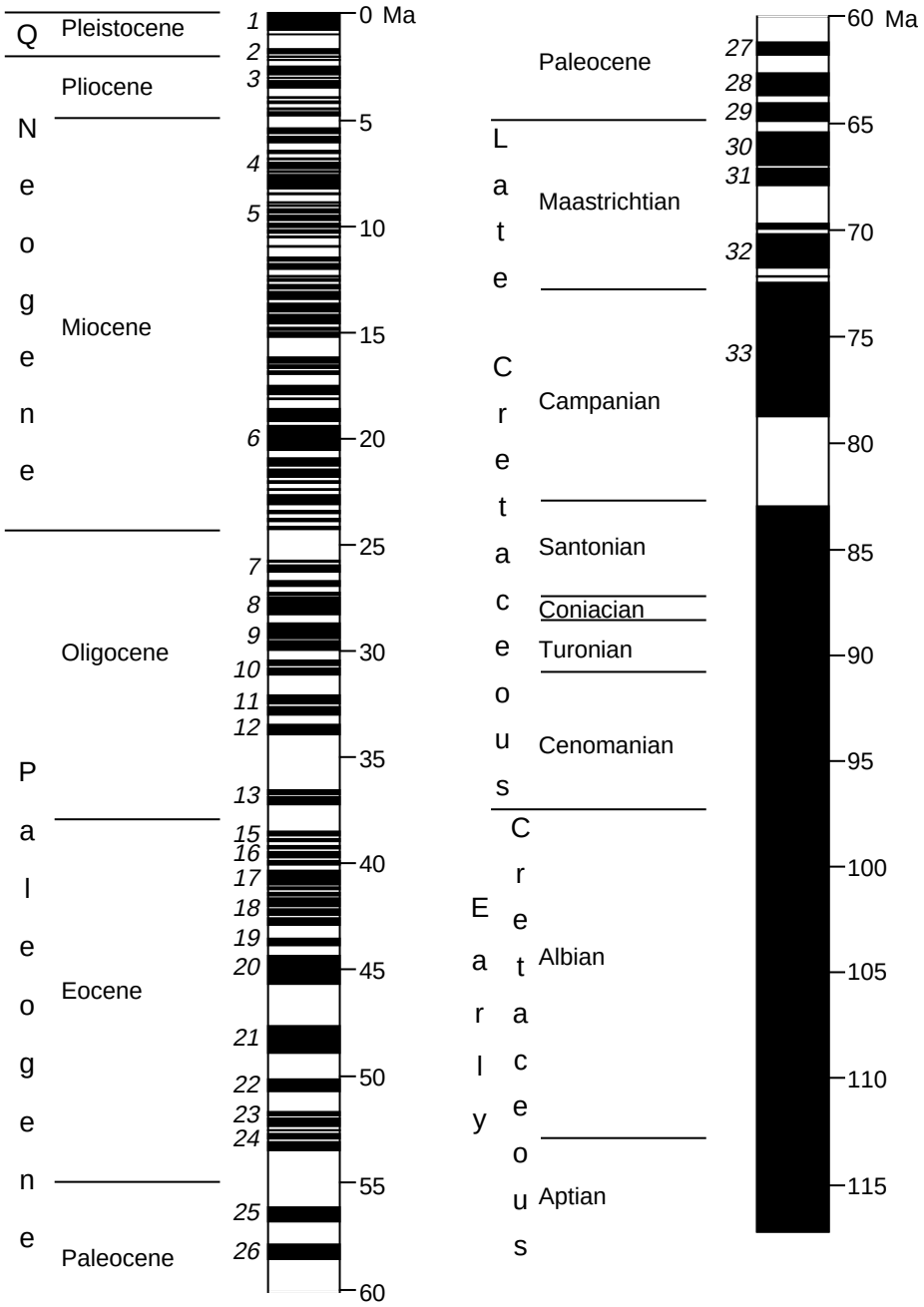

Figure 9.9 Geomagnetic polarity time scale of Cox (1982) from 0 to 118 Ma. Geologic time divisions are shown to the left of the polarity column; magnetic anomaly numbers (polarity chron numbers) are shown in italics at the left of the polarity column; age (in Ma) is shown by the scale to the right of the polarity column. Redrawn from Cox (1982).

Two points should be made about the Late Cretaceous and Cenozoic polarity time scale.

1. Although different approaches have been used in developing polarity time scales, the differences between recent time scales are minor. At least for the Cenozoic, we can conclude that absolute ages of magnetic polarity chrons are known to a precision of ±2 m.y. It is also important to realize that relative age determinations within a particular polarity time scale are known to much better precision than are the absolute ages. The precision of relative age determinations can approach 10^4 yr.

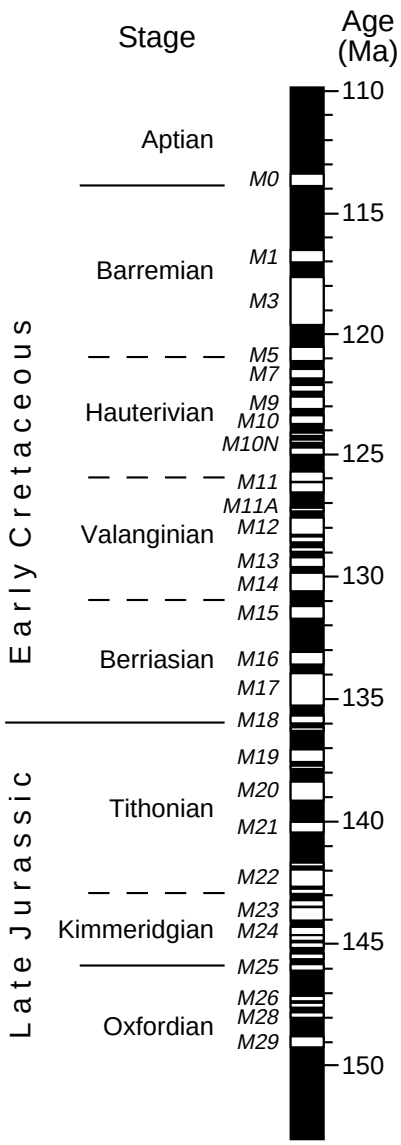

Figure 9.10 Geomagnetic polarity time scale of Lowrie and Ogg (1986) for the Late Jurassic and Early Cretaceous. Geologic time divisions are shown to the left of the polarity column, and the absolute age scale is given to the right of the column; "M anomaly" designations of reversed polarity chrons are given in italics at the left of the polarity column. Redrawn from Lowrie and Ogg (1986).

2. A major feature of the geomagnetic polarity time scale in the Cretaceous is the *Cretaceous normal-polarity superchron*, during which the geomagnetic field was of constant normal polarity. On the Cox (1982) time scale, this interval has absolute age limits of 118 and 83 Ma; the geomagnetic field did not reverse polarity for ~35 m.y.! McFadden and Merrill (1986) present an interesting discussion of polarity superchrons, changes in reversal frequency, and possible links to mantle convection.

The Late Mesozoic

Marine magnetic anomalies have also been mapped above Late Jurassic and Early Cretaceous oceanic crust. These are the "M anomalies," in which "M" stands for Mesozoic. Again, prominent positive magnetic anomalies have been numbered. Because of large-scale plate motions since the Late Jurassic, the positive M anomalies are produced by underlying oceanic crust with reversed polarity. A recent GPTS for the Late Jurassic and Early Cretaceous is shown in Figure 9.10. Notice that the labeled polarity chrons are reversed-polarity intervals. For example, polarity chron M17 is the reversed-polarity interval in the early portion of the Berriasian stage of the Early Cretaceous.

As with geologic time scales, our knowledge of the GPTS for the Late Jurassic and Early Cretaceous is less precise than for the Cenozoic. Data from primarily three sources are refining biostratigraphic calibration of this portion of the polarity time scale:

1. Analysis of marine magnetic anomaly profiles and paleontological dating of sediment in DSDP and ODP cores have provided important information about the biostratigraphic age of particular polarity chrons.

2. Magnetostratigraphic studies on ODP cores obtained with the advanced piston-coring system have provided critical information about placement of magnetic polarity chrons within biostratigraphic stages of the mid-Mesozoic.

3. Magnetostratigraphic studies of "stratotype sections" in Europe have also provided critical data leading to refinements in the geomagnetic polarity time scale.

In addition to uncertainties in biostratigraphic calibration, absolute age calibration of the Late Jurassic and Early Cretaceous polarity time scale is uncertain. The absolute ages of some stage boundaries in the mid-Mesozoic differ between various geologic time scales by as much as 10 m.y. So the absolute age of polarity chrons in this geologic time interval are known to only about ±5 m.y. But this is a topic of active

research, and biostratigraphic and absolute age calibrations of the Late Jurassic and Early Cretaceous polarity time scale should be significantly advanced in the coming years.

Early Mesozoic, Paleozoic, and Precambrian

The oldest substantial portions of oceanic crust remaining in ocean basins are Late Jurassic in age. So the determination of the GPTS for older intervals must be done by paleomagnetic studies of exposed stratigraphic sections on land. Accordingly, our knowledge of the polarity time scale for Early Mesozoic and older times is much less refined than for the Late Mesozoic and Cenozoic. The status of knowledge is summarized in Figure 9.11.

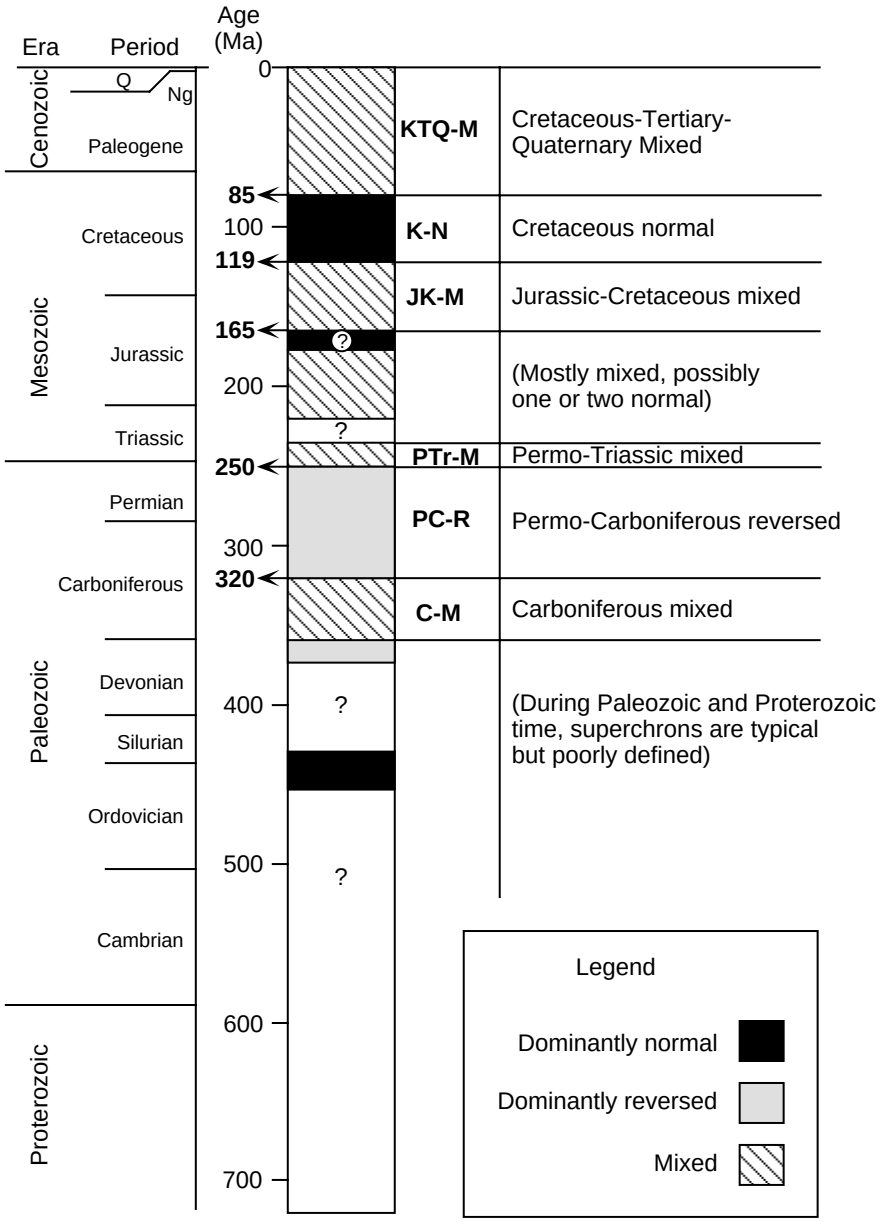

Figure 9.11 Polarity bias superchrons during the Proterozoic and Phanerozoic. Geologic time divisions are shown to the left of the polarity bias column; Q = Quaternary; Ng = Neogene; absolute age is shown to the left of the polarity bias column with age limits of polarity superchrons shown in bold type; names of polarity bias superchrons are given to the right of the column. Redrawn from Cox (1982).

The best-documented feature of the polarity time scale for the Paleozoic is the *Permo–Carboniferous reversed-polarity superchron*, an interval of (almost?) constant reversed polarity lasting for ~70 m.y. from the mid-Carboniferous through most of the Permian. The Permo-Carboniferous reversed-polarity superchron is also known as the *Kiaman interval*. This interval was preceded and followed by intervals of frequent geomagnetic reversals. Stratigraphic correlations between widely separated Paleozoic sections are often difficult to establish by using biostratigraphy. So defining the stratigraphic limits of the Permo-Carboniferous reversed-polarity interval has been used to accomplish intercontinental stratigraphic correlations within the Late Paleozoic.

Aside from a reversed-polarity superchron in the Devonian and a normal-polarity superchron from Late Ordovician through Early Silurian, the pattern of polarity reversals in the Early Paleozoic and Proterozoic is poorly known. Accurate determination of the polarity time scale in this time interval is a major challenge. However, polarity stratigraphy can still serve as a useful stratigraphic correlation technique even though the biostratigraphic and absolute age calibrations are rudimentary (e.g., Kirschvink, 1978).

MAGNETIC POLARITY STRATIGRAPHY

This section starts with discussion of general principles of magnetostratigraphy. In the remainder of the chapter, case histories of magnetic polarity stratigraphy applied to geochronologic problems are presented. The specific examples are applications to Neogene continental sedimentary sequences, but the procedures and principles apply to magnetostratigraphic studies in all sedimentary environments. Through study of these case histories, you will gain an appreciation of strategies used in magnetostratigraphic investigations and of the powers and limitations of magnetic polarity stratigraphy.

Some general principles

In most applications, the primary objective is to provide an age estimate for an event (or series of events) occurring within a sequence of sedimentary rocks. A correlation is usually sought between an observed magnetic polarity zonation in a stratigraphic section and the geomagnetic polarity time scale. In essence, the objective is to determine a pattern of polarity zones that provides a “fingerprint” of a particular interval of the GPTS. The strength of correlation of an observed magnetic polarity zonation to the GPTS depends on several factors including (1) the quality of paleomagnetic data used to define the polarity of each sampled stratigraphic horizon, (2) stratigraphic coverage of sites used to define the magnetic polarity zones, and (3) uniqueness of matching between the pattern of magnetic polarity zones and the sequence of magnetic polarity chrons of the GPTS.

Unambiguous determination of the polarity of the ChRM is the major experimental requirement for magnetic polarity stratigraphy. Consistency of polarity determinations between stratigraphically adjacent sites usually allows clear determination of the polarity zonation. But if a large percentage of sites contain complex magnetizations, the clarity of the polarity zonation is compromised. Normal-polarity sites that are stratigraphically isolated should always be viewed with some suspicion; the NRM could be dominated by an unremoved normal-polarity overprint.

Fine-grained lithologies (claystones, fine siltstones, and mudstones) are generally preferred. These fine-grained sediments acquire DRM more efficiently than coarser lithologies. Also, fine-grained sedimentary layers usually have low permeability and are less susceptible to acquisition of secondary CRM. Collection of a variety of sedimentary rocks (sometimes including unconsolidated lithologies) often requires use of oriented block samples.

Sampling strategies should provide efficient determination of polarity zonation. On the one hand, collecting single samples from closely spaced sedimentary horizons may maximize stratigraphic coverage with a given number of samples. On the other hand, replicate samples from within a horizon can provide critical evaluation of reliability of polarity determinations. For most applications, the compromise strategy of collect-

ing three or four samples from each paleomagnetic site is appropriate. This is the minimum number of samples required for application of statistical analysis (usually Fisher statistics). Often a classification of the quality of site-mean polarity determinations is developed on the basis of multiple samples per site (see the example discussions below).

The stratigraphic separation between paleomagnetic sites depends on the sedimentary environment and the age of the section. For continental sediments in a fluvial environment, sediment accumulation rates are typically 10 to 100 m/m.y. (Sadler, 1981). With a polarity reversal rate of ~4/m.y. during the Neogene, a typical polarity zone is expected to have a thickness of ~10 m. So a stratigraphic separation of 3 m between sites generally allows resolution of the polarity zonation. In pelagic environments, sediment accumulation rate is generally <10 m/m.y., and <0.5-m stratigraphic spacing of sites is recommended to allow resolution of important polarity zones.

The uniqueness of correlation between an observed polarity zonation and the GPTS depends on the number and pattern of polarity zones. A useful analogy is identification of crime suspects by fingerprint. A whole thumbprint is likely to hold up in court, but a quarter thumbprint will rarely provide convincing evidence. In the examples presented below, you will see that 10 to 20 polarity zones in a stratigraphic section usually have a pattern that can be unambiguously correlated to the GPTS. Fewer zones may be sufficient if appropriate independent age control is available.

With a reversal rate of ~4/m.y. during the Neogene, the time span represented by a stratigraphic section should be ≥2 m.y. to provide effective correlation to the GPTS. For typical sediment accumulation rates, a continental sedimentary sequence ≥100 m thick is generally required, but a pelagic sequence that is only a few meters thick may suffice (e.g., Figure 9.3). With the lower rate of polarity reversals in the Late Cretaceous and Paleogene, continental sedimentary sections of ≥500 m thickness and pelagic sequences of ≥100 m are generally required for convincing correlation to the GPTS. (Note that the Gubbio section of Figures 9.6 and 9.7 has a thickness >150 m.)

Mathematical cross-correlation techniques have been used to evaluate correlations between magnetic polarity zonations and the GPTS. But correlations are often made convincing by independent age constraints that are difficult to quantify. For example, the fossils at a particular stratigraphic level may be Late Miocene in age. In evaluating alternative correlations, only those placing the fossil level within the Late Miocene portion of the GPTS are reasonable. Isotopic age determinations can also provide tie points, facilitating correlation. In the end, the pattern matching between the observed polarity zonation and the GPTS <u>plus</u> the independent age constraints make a correlation either convincing or ambiguous.

These general principles are brought into focus only by the presentation of specific examples. As we examine the case histories below, keep the general principles in mind by asking the following questions:

1. Do the paleomagnetic data clearly determine the polarity of ChRM at each site?
2. Is the stratigraphic coverage sufficient to delineate the polarity zonation?
3. Considering the independent age constraints, how convincingly does the magnetic polarity zonation correlate to the GPTS?

The Pliocene–Pleistocene St. David Formation

Our first example is an application of magnetostratigraphy to geochronologic calibration of North American land mammal ages. The Cenozoic biostratigraphy of continental deposits is based on mammalian evolution, whereas biostratigraphy in the marine system is based on evolution of invertebrates. Correlation between these biostratigraphic systems depends on stratigraphic intertonguing, occasional isotopic age determinations, and magnetic polarity stratigraphy. Johnson et al. (1975) accomplished an important step in geochronologic calibration of Neogene North American land mammal ages through magnetostratigraphic study of continental deposits in southeastern Arizona. Their pioneering effort led to many similar applications of magnetic polarity stratigraphy to geochronologic problems involving continental sedimentary sequences.

The San Pedro Valley of southeastern Arizona is in the Basin and Range physiographic province, which has experienced crustal extension during the Late Cenozoic. The Miocene to Pleistocene valley fill deposits of the St. David Formation are dominated by lacustrine and fluvial continental deposits. Fossil mammal assemblages include the Benson fauna belonging to the Blancan Land Mammal Age and the Curtis Ranch fauna belonging to the younger Irvingtonian Land Mammal Age. The major objective of the magnetostratigraphic research was to produce a detailed correlation between these Pliocene–Pleistocene land mammal ages and the marine biozonations by defining the position of the Blancan and Irvingtonian land mammal ages within the GPTS.

The 150-m-thick Curtis Ranch section was the major stratigraphic section for which the magnetic polarity zonation was determined (Figure 9.12). Three block samples were collected at each of 81 paleomagnetic sites separated by an average stratigraphic spacing of 3.3 m. Strong-field thermomagnetic analysis of magnetic separates indicated that magnetite and titanomagnetite are the dominant ferromagnetic minerals. Claystones proved to contain the most stable NRM with the ChRM interpreted as detrital in origin. AF demagnetization to peak fields of 100 to 150 Oe (10 to 15 mT) successfully removed secondary VRM, isolating the ChRM, which had an average intensity of 1×10^{-5} G (1×10^{-2} A/m). The mean directions for the normal- and reversed-polarity sites passed the reversals test, adding confidence in the polarity determinations.

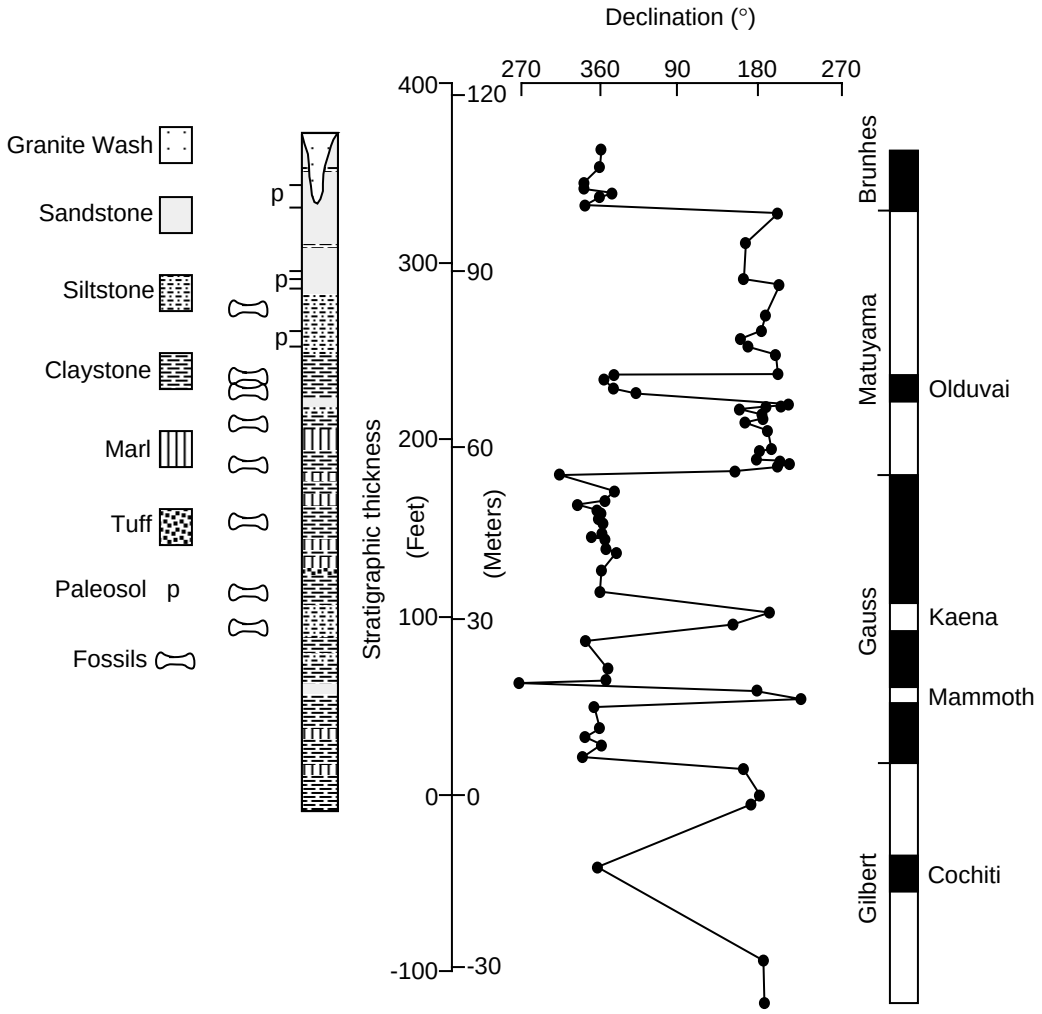

Figure 9.12 Site-mean ChRM declination versus stratigraphic position at Curtis Ranch, San Pedro Valley, Arizona. The interpreted polarity column and correlations to the GPTS are shown at the right. Redrawn from Johnson et al. (1975) with permission from the Geological Society of America.

As seen in Figure 9.12, 12 polarity zones were defined within the Curtis Ranch section. An important age constraint was provided by a K-Ar date of 2.5 ± 0.4 Ma from a volcanic ash within the reversed-polarity zone at the 60- to 70-m stratigraphic level. This reversed-polarity zone thus is best correlated with the early portion of the Matuyama epoch, which has absolute age limits of 2.43 Ma and 1.86 Ma on the GPTS used by Johnson et al. (1975). With that correlation accomplished, the pattern of polarity zones of the Curtis Ranch section convincingly correlates to the GPTS from the late Gilbert epoch into the Brunhes epoch. (Notice that the correlation shown in Figure 9.12 implies that the Reunion events and the Jaramillo event were not detected in the Curtis Ranch section. We will return to this point below.)

In Figure 9.13, fossil levels within the St. David Formation are shown within their respective magnetic polarity zones, which have been correlated to the GPTS. All the absolute age calibration of the GPTS thus can be used to provide absolute age estimates for the faunal levels within this continental sedimentary sequence in which little directly datable material was present. The *Lepus* faunal datum is the first appearance of a definitive Irvingtonian land mammal (rabbit), and the local boundary between the Blancan and Irvingtonian land mammal ages occurs just prior to the Olduvai event. This geochronologic calibration places the Blancan/Irvingtonian boundary very close to the marine Pliocene/Pleistocene boundary (Berggren et al., 1985). Johnson et al. (1975) thus accomplished the detailed correlation between Late Cenozoic land mammal ages and marine biozonations that they sought.

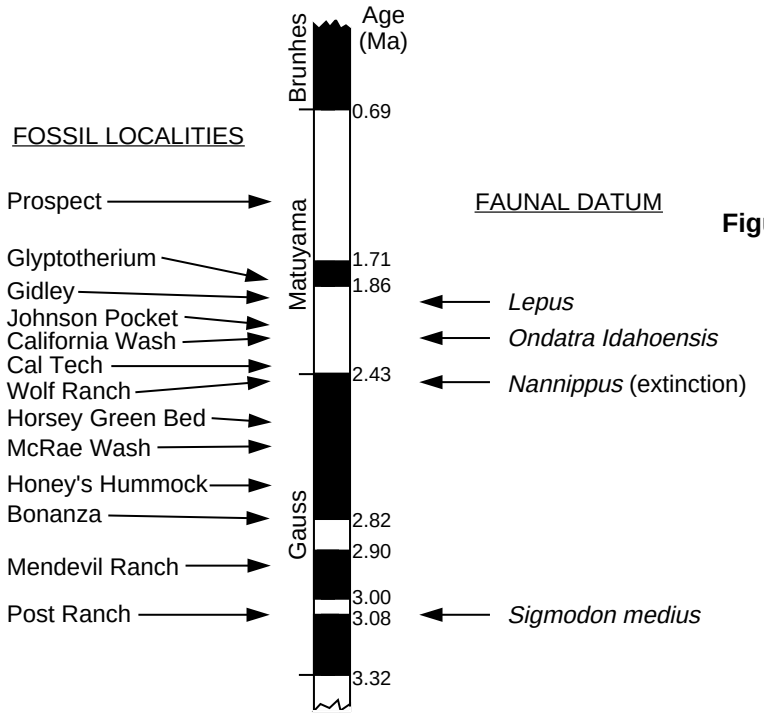

Figure 9.13 Occurrences of fossil-mammal localities in San Pedro Valley with respect to the GPTS. Absolute ages of polarity intervals are indicated on the right side of the polarity column. Redrawn from Johnson et al. (1975) with permission from the Geological Society of America.

As illustrated by the "missing" Curtis Ranch polarity zones corresponding to the Jaramillo and Reunion events (Figure 9.12), polarity stratigraphies often lack polarity zones corresponding to short-duration polarity intervals. Sometimes, as in the Curtis Ranch section, the stratigraphic spacing of sites does not permit detection of short-duration polarity intervals (Johnson and McGee, 1983). It is also possible that a hiatus in sediment accumulation occurred during the time span of a short-duration polarity interval. The discontinuity of sediment accumulation has important implications for magnetostratigraphy and can be quantified by the approach of *stratigraphic completeness*. For discussions of stratigraphic completeness and magnetostratigraphy, see May et al. (1985) and Badgley et al. (1986).

Siwalik Group deposits

The Siwalik Group of northwest India and Pakistan is a sequence of Neogene continental sediments shed from the Himalayas onto the Indian subcontinent during its collision with southern Asia. Because this sequence has been a rich source of Miocene fossil mammals, detailed correlation between fossil localities within the Siwalik deposits and geochronologic calibration of the sedimentary sequence is important to deciphering the evolution of Asian mammals, including primate lineages.

Our next magnetostratigraphic example is part of a large effort to accomplish geochronologic calibration of the Siwalik deposits. Johnson et al. (1985) examined the magnetic polarity stratigraphy of sediments exposed near Chinji Village, Pakistan. In this location, the Siwalik sequence overlies Eocene marine limestone. In stratigraphic order, the formations of the homoclinal sequence are (1) alternating sandstones and mudstones of the Kamlial Formation (in some localities called the Murree Formation), (2) greenish-gray sandstones and brown-red mudstones of the Chinji Formation, (3) multistoried green-gray sandstones of the Nagri Formation, and (4) brown silts of the Dhok Pathan Formation. This stratigraphic sequence is exposed in two major drainages: a lower section in Chita Parwala Kas and an upper section in Gabhir Kas.

Although rock colors range from gray to red, Siwalik sediments are “red beds” in the sense that the NRM is carried by hematite. Tauxe et al. (1980) performed detailed rock-magnetic analyses to determine the origin of NRM components. The NRM properties divided the lithologies into two broad categories: “gray sediments” and “red sediments.” Progressive thermal demagnetization showed that gray sediments have a component of NRM with low blocking temperatures (T_B) up to ~400°C and a ChRM component with T_B up to 675°C. Both components are carried by specular hematite, and the low T_B component is quite clearly a VRM. The red sediments have two NRM components in addition to the low T_B VRM. Vector end-point diagrams of progressive thermal demagnetization revealed that the trajectory of vector end points often reversed trend between 525° and 600°C prior to final trajectory to the origin at 680°C. This indicated removal of an NRM component with direction antiparallel to the ChRM.

Tauxe et al. (1980) did coercivity spectrum analysis (Chapter 4) on untreated samples and on samples leached with acid to remove the red pigment. They demonstrated that the pigment had T_B in the 525 to 600°C range and that the ChRM component was carried by specular hematite. The NRM component with direction antiparallel to the ChRM (and with T_B from 525° to 600°C) thus was interpreted as CRM carried by the red pigment. Formation of this NRM component postdates the ChRM formation by at least one polarity reversal.

A conglomeratic layer was located within the Siwalik sequence. The ChRM component of sediment cobbles was shown to be carried by specular hematite and to pass a conglomerate test. Tauxe et al. (1980) thus argued that the ChRM must have been acquired as either a DRM or an early-formed CRM. These important rock-magnetic observations demonstrate that ChRM directions obtained through thermal demagnetization to 600°C can be reliably used to determine the polarity sequence during deposition of Siwalik sediments.

Johnson et al. (1985) collected three block samples at 159 paleomagnetic sites distributed through the two stratigraphic sections and subjected all samples to thermal demagnetization at 600°C. The site-mean results were broken into two classes according to within-site clustering of ChRM directions. Sites with clustering that was significant from random (5% significance level) were designated “class A.” Sites with clustering of ChRM directions that was not significant from random but in which the ChRM polarity of two samples agreed were designated “class B.” In the stratigraphic sections near Chinji Village, there were 99 class A sites, 37 class B sites, and 23 sites that yielded ambiguous results and were rejected. The means of the class A normal- and reversed-polarity groups passed the reversals test.

The magnetic polarity stratigraphies established for the Chita Parwala Kas and Gabhir Kas sections are shown in Figure 9.14. The site-mean VGP latitudes quite cleanly define the polarity zones. Two sandstone layers were traced between the sections and are shown connecting the lithostratigraphic sec-

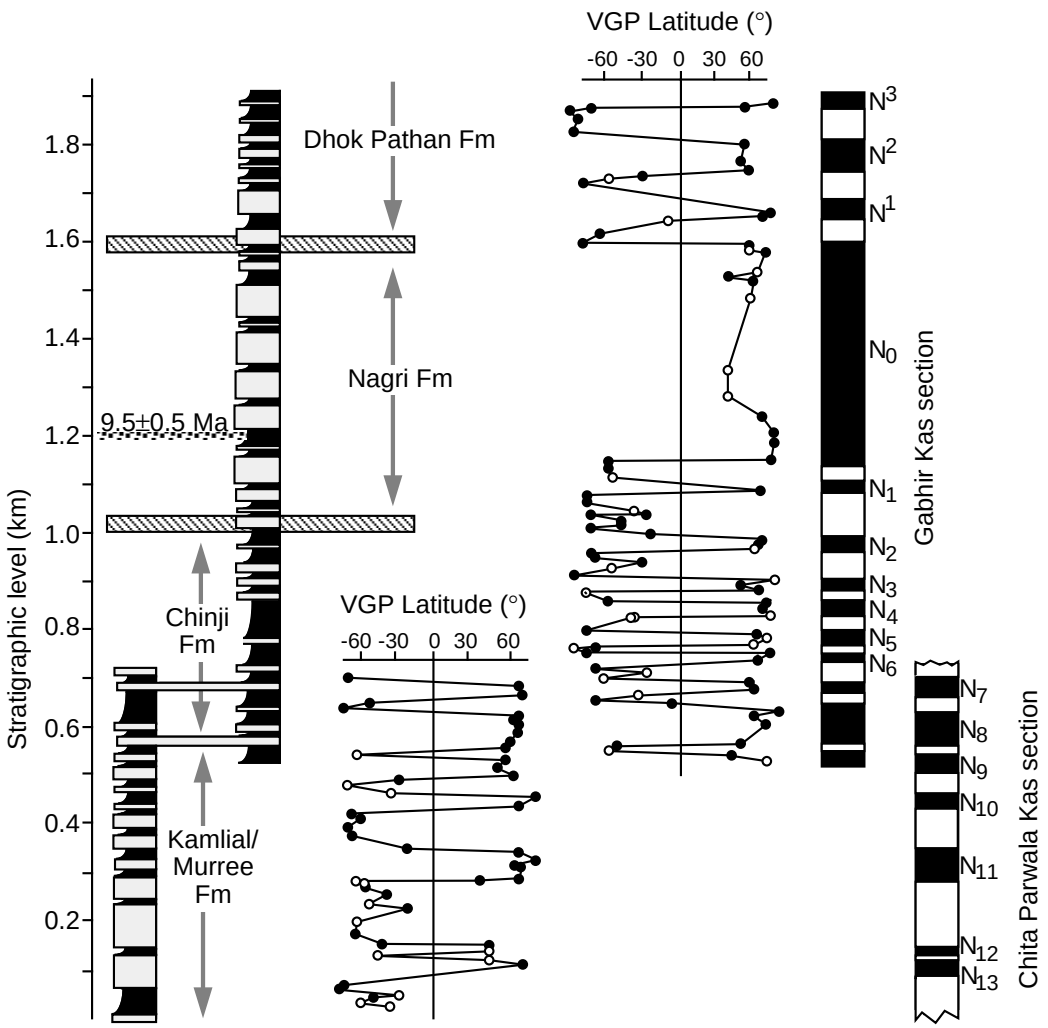

Figure 9.14 Stratigraphic correlation and polarity stratigraphy of Chita Parwala and Gabhir Kas sections. Resistant sandstones are shown by the stippled pattern in the stratigraphic section; finer-grained lithologies are shown in black; tracer sandstone units are shown connecting lithostratigraphic sections; VGP latitudes for class A sites are shown by solid circles; VGP latitudes for class B sites are shown by open circles; the interpreted magnetic polarity zonation is shown at the right. Redrawn from Johnson et al. (1985) with permission from the *Journal of Geology*. Copyright© 1985 by The University of Chicago.

tions in Figure 9.14. The lithologic correlation is corroborated by the magnetic polarity zonations; normal-polarity zones N_7 and N_8 are found in both sections. The magnetic polarity zonations from the two sections were combined into a composite magnetostratigraphic section for Siwalik deposits in this region.

The composite magnetic polarity zonation and its correlation to the GPTS are shown in Figure 9.15. A fission-track date of 9.5 ± 0.5 Ma from an ash deposit within the Nagri Formation allows the thick normal-polarity zone containing the ash to be securely correlated with chron 5 of the GPTS. Also, the polarity pattern and dominance of reversed-polarity within the lower portion of the section correlates well with the polarity pattern of chrons 5Br through 5Cr. Considering the age constraint provided by the fission-track date and the overall matching of the pattern of polarity zones with that of the GPTS in the 18 to 8-Ma interval, the correlation of Figure 9.15 is reasonably convincing. From this magnetostratigraphic analysis, Johnson et al. (1985) estimated absolute ages of formational boundaries and fossil localities within these Siwalik deposits. The Kamlial/Chinji boundary has an estimated

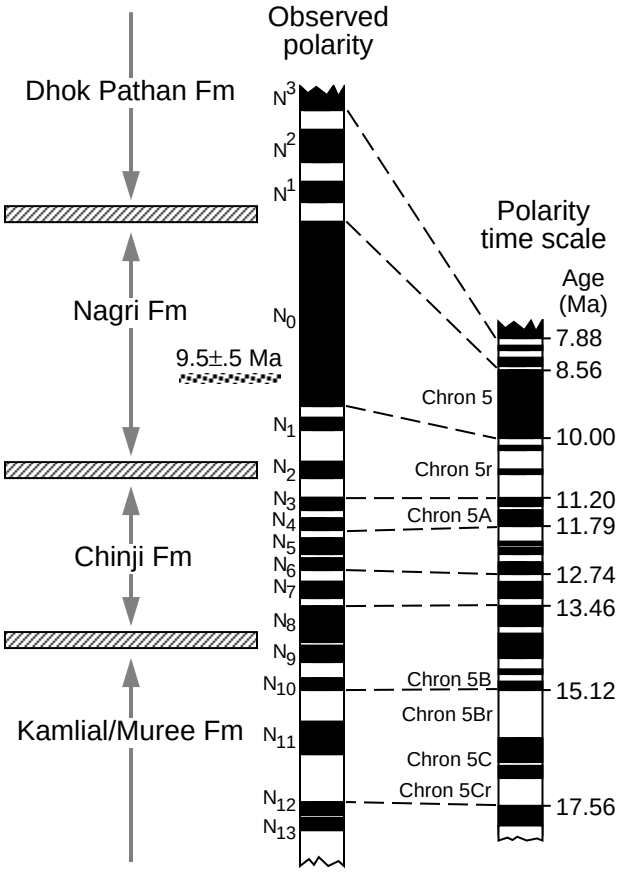

Figure 9.15 Correlation of magnetic polarity zonation of Siwalik deposits near Chinji Village, Pakistan, with the of Mankinen and Dalrymple (1979); the "chron" numbering system is from Cox (1982). Redrawn from Johnson et al. (1985) with permission from the Journal of Geology. Copyright© 1985 by The University of Chicago.

age of 14.3 Ma; the Chinji/Nagri boundary is estimated at 9.8 Ma; and an estimate of 8.5 Ma is made for the Nagri/Dhok Pathan boundary.

An interesting additional observation is shown in Figure 9.16. The age indicated by the magnetostratigraphy and fission-track dating is graphed against stratigraphic level, with slope indicating rate of sediment accumulation. The lower portion of the section has a reasonably constant rate of sediment accumulation of 0.12 m/1000 yr. But the upper portion with age <11 Ma has a higher rate of 0.30 m/1000 yr. This change in sediment accumulation rate also correlates with a marked increase in metamorphic detritus (especially blue-green hornblendes). The tectonic interpretation is that the rate of sediment accumulation accelerated at ~11 Ma because of unroofing of metamorphic rocks in the source region. Indeed, uplift of 10 km since 10 Ma has been documented for the likely source region, the Nanga Parbat-Hunza region of the Himalayas.

The tectonic and sedimentologic implications of the magnetostratigraphic work of Johnson et al. (1985) are best summarized in their concluding paragraph:

> In the long-range view then, the Siwalik sequence in the Chinji Village area represents just one ephemeral stage in a dynamic system of landforms, sediments, and tectonics. In the course of its northward drift the Indian Plate has acted like a conveyor belt, bringing a continuous series of depositional sites, including the Chinji Village area, along with it. During its northward ride, the Chinji Village site has been converted slowly from a karst terrane into a depositional terrane, and most recently into a thrust belt and source terrane. Our chronologic data from Chinji Village suggest that the life cycle for each depositional site spans some 20 m.y.

Siwalik sedimentology

The final example application of magnetic polarity stratigraphy is the sedimentological study of Siwalik Group sediments near Dhok Pathan, Pakistan, by Behrensmeyer and Tauxe (1982). In this region, shown

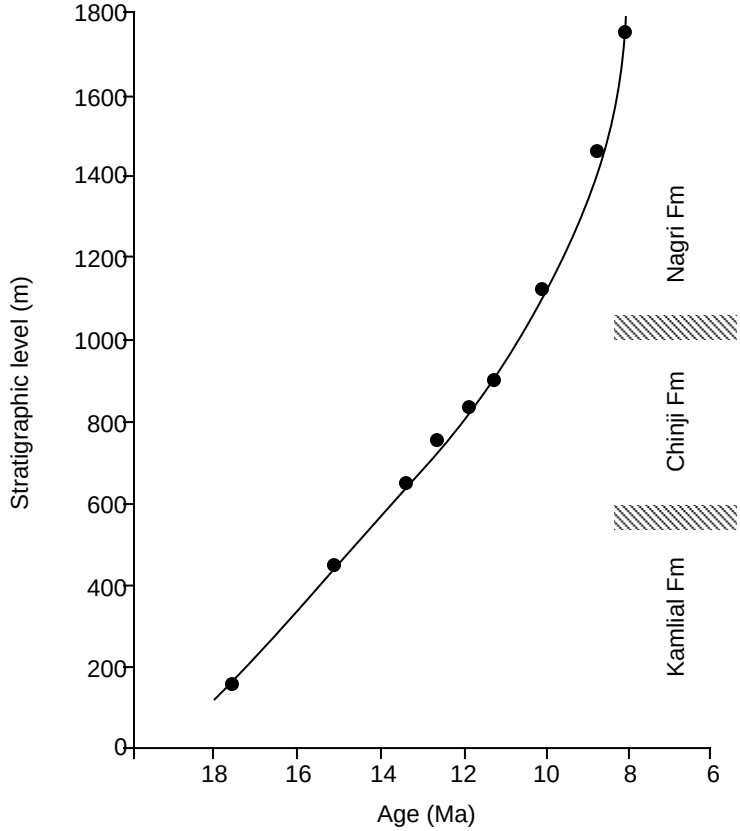

Figure 9.16 Sediment accumulation history of Siwalik deposits near Chinji Village. Data points are boundaries between identified magnetic polarity chrons; the slope of the curve is the sediment accumulation rate. Redrawn from Johnson et al. (1985) with permission from the *Journal of Geology*. Copyright© 1985 by The University of Chicago.

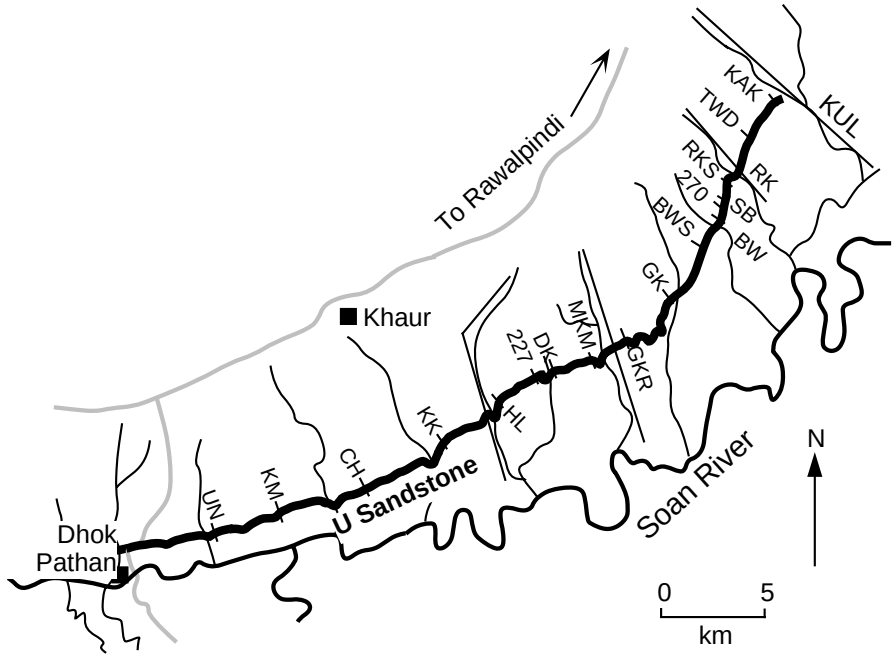

Figure 9.17 Stratigraphic sections of Middle Siwalik deposits near Khaur, Pakistan. The heaviest black line shows the outcrop of U Sandstone; the medium black line shows the course of Soan River; the thin, sinuous black lines show canyons cutting across the strike of deposits; stippled lines indicate roads; initials label stratigraphic sections located by straight black lines and shown in Figure 9.18; the region is within Potwar Plateau. Redrawn from Behrensmeyer and Tauxe (1982).

in Figure 9.17, the Nagri Formation is characterized by laterally extensive sheet sandstones, while the Dhok Pathan Formation is characterized by siltstones and claystones. On a gross scale, the Dhok Pathan Formation overlies the Nagri Formation. But using a particular magnetic polarity zone boundary as an isochronous marker, Behrensmeyer and Tauxe showed that the formational boundary is a complex interfingering of two fluvial systems.

Previous magnetic polarity studies by Tauxe and Opdyke (1982) provided correlation of the magnetic polarity zonation of the Nagri and Dhok Pathan formations in this region to the GPTS. The paleomagnetic data were similar to those reported by Johnson et al. (1985), and a similar "class" designation was used for reliability of polarity determinations. The correlation provided an absolute age estimate of 8.1 Ma for the boundary between normal-polarity zone DN4 and the overlying reversed-polarity zone DR4. Excellent exposures of the Middle Siwalik group north of the Soan River allowed paleomagnetic sampling of a 40 m stratigraphic interval spanning the DN4-DR4 boundary in closely spaced sections over a distance of 40 km (Figure 9.17). The top of a continuous sheet sandstone body (U Sandstone) was used as a stratigraphic datum for correlation between sections.

A southwest-to-northeast cross section of the major lithologies and the paleomagnetic polarity determinations is shown in Figure 9.18. With an average sediment accumulation rate of 0.52 m/1000 yr and sedimentologic evidence that the boundary is not marked by a hiatus, the DN4-DR4 boundary approximates an isochronous horizon. This cross-sectional mapping of the DN4-DR4 "time line" provides the magnetostratigraphic proof of a basic concept in stratigraphy and sedimentology: the intertonguing of two geologic formations and the time-transgressive nature of the formational contact.

In this particular case, the intertonguing of the Nagri and Dhok Pathan formations is the result of interfingering between two contemporaneous fluvial systems. On the southwest, the dominant system deposited widespread blue-gray sheet sandstones characteristic of the Nagri Formation. To the northeast, the dominant system deposited silt and clay with occasional restricted lenses of buff-colored sandstone. Through use of the DN4-DR4 isochron, Behrensmeyer and Tauxe (1982) developed a model for the tectonic and hydrologic influences on the interfingering of the two depositional systems.

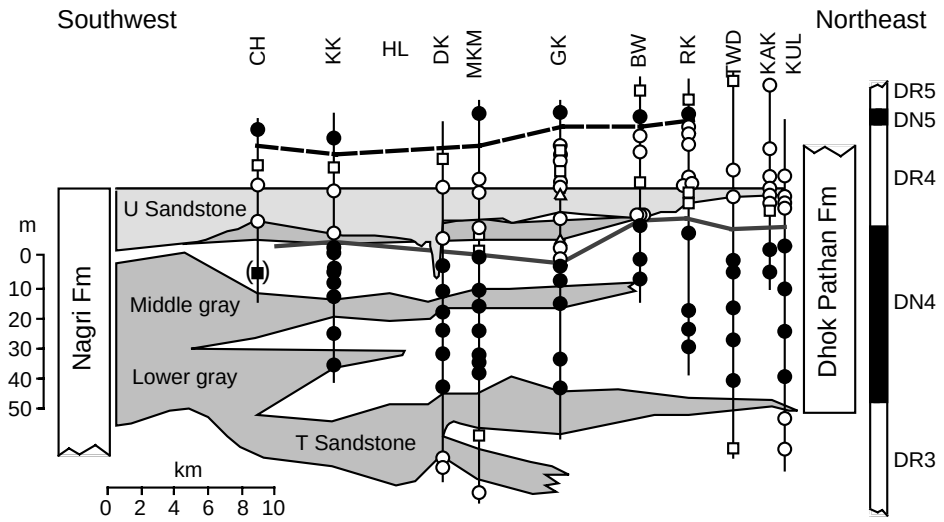

Figure 9.18 Magnetostratigraphic correlation of DN4-DR4 polarity boundary along the strike of the U Sandstone. Sheet sandstones on the southwest side of the cross section are assigned to the Nagri Formation, while silts and clays (shown by white) are characteristic of the Dhok Pathan Formation to the northwest; the top of the U Sandstone is used as a horizontal reference; circles indicate class A paleomagnetic sites; squares indicate class B sites; triangles indicate class C sites (within-site clustering of ChRM significant from random after AF demagnetization); black indicates normal polarity; white indicates reversed polarity; the bold stippled line indicates the position of the DN4-DR4 polarity boundary. Redrawn from Behrensmeyer and Tauxe (1982).

REFERENCES

L. W. Alvarez, W. Alvarez, F. Asaro, and H. V. Michel, Extraterrestrial cause for the Cretaceous–Tertiary extinction, *Science*, v. 208, 1095–1108, 1980.

C. Badgley, L. Tauxe, and F. L. Bookstein, Estimating the error of age interpolation in sedimentary rocks, *Nature*, v. 319, 139–141, 1986.

A. K. Behrensmeyer and L. Tauxe, Isochronous fluvial systems in Miocene deposits of northern Pakistan, *Sedimentology*, v. 29, 331–352, 1982.

W. A. Berggren, D. V. Kent, J. J. Flynn, and J. A. Van Couvering, Cenozoic geochronology, *Geol. Soc. Am. Bull.*, v. 96, 1407–1418, 1985.

A. Cox, *Plate Tectonics and Geomagnetic Reversals*, W. H. Freeman and Co., San Francisco, 702 pp., 1973.

A. Cox, Magnetostratigraphic time scale, In: *A Geologic Time Scale*, ed. W. B. Harland et al., Cambridge University Press, Cambridge, England, pp. 63–84, 1982.

A. Cox, R. R. Doell, and G. B. Dalrymple, Geomagnetic polarity epochs and Pleistocene geochronometry, *Nature*, v. 198, 1049–1051, 1963.

A. Cox, R. R. Doell, and G. B. Dalrymple, Geomagnetic polarity epochs, *Science*, v. 143, 351–352, 1964.

A. Cox, R. R. Doell, and G. B. Dalrymple, Radiometric time-scale for geomagnetic reversals, *Quart. J. Geol. Soc.*, v. 124, 53–66, 1968.

K. M. Creer, P. Tucholka, and C. E. Barton, *Geomagnetism of Baked Clays and Recent Sediments*, Elsevier, Amsterdam, 324 pp., 1983.

R. R. Doell and G. B. Dalrymple, Geomagnetic polarity epochs: A new polarity event and the age of the Brunhes–Matuyama boundary, *Science*, v. 152, 1060–1061, 1966.

W. Glen, *The Road to Jaramillo*, Stanford University Press, Stanford, Calif., 459 pp., 1982.

E. A. Hailwood, *Magnetostratigraphy*, Special Report No. 19, The Geological Society, Blackwell Scientific Publications, Oxford, England, 84 pp., 1989.

J. R. Heirtzler, G. O. Dickson, E. M. Herron, W. C. Pitman, III, and X. Le Pichon, Marine magnetic anomalies, geomagnetic field reversals, and motions of the ocean floor and continents, *J. Geophys. Res.*, v. 73, 2119–2136, 1968.

N. M. Johnson and V. E. McGee, Magnetic polarity stratigraphy: Stochastic properties of data, sampling problems, and the evaluation of interpretations, *J. Geophys. Res.*, v. 88, 1213–1221, 1983.

N. M. Johnson, N. D. Opdyke, and E. H. Lindsay, Magnetic polarity stratigraphy of Pliocene–Pleistocene terrestrial deposits and vertebrate faunas, San Pedro Valley, Arizona, *Geol. Soc. Am. Bull.*, v. 86, 5–12, 1975.

N. M. Johnson, J. Stix, L. Tauxe. P. F. Cerveny, and R. A. K. Tahirkheli, Paleomagnetic chronology, fluvial processes, and tectonic implications of the Siwalik deposits near Chinji Village, Pakistan, *J. Geol.*, v. 93, 27–40, 1985.

J. L. Kirschvink, The Precambrian–Cambrian boundary problem: Magnetostratigraphy of the Amadeus Basin, Central Australia, *Geol. Mag.*, v. 115, 139–150, 1978.

J. L. La Brecque, D. V. Kent, and S. C. Cande, Revised magnetic polarity time scale for Late Cretaceous and Cenozoic time, *Geology*, v. 5, 330–335, 1977.

W. Lowrie, Magnetic polarity time scales and reversal frequency, In: *Geomagnetism and Paleomagnetism*, ed. F. J. Lowes, D. W. Collinson, J. H. Parry, S. K. Runcorn, D. C. Tozer, and A. Soward, Kluwer Academic Publishers, Dordrecht, Netherlands, pp. 155–183, 1989.

W. Lowrie and W. Alvarez, Upper Cretaceous–Paleocene magnetic stratigraphy at Gubbio, Italy, III. Upper Cretaceous magnetic stratigraphy, *Geol. Soc. Am. Bull.*, v. 88, 374–377, 1977.

W. Lowrie and W. Alvarez, One hundred million years of geomagnetic polarity history, *Geology*, v. 9, 392–397, 1981.

W. Lowrie and J. G. Ogg, A magnetic polarity time scale for the Early Cretaceous and Late Jurassic, *Earth Planet. Sci. Lett.*, v. 76, 341–349, 1986.

E. A. Mankinen and G. B. Dalrymple, Revised geomagnetic polarity time scale for the interval 0-5 m.y. B.P., *J. Geophys. Res.*, v. 84, 615–626, 1979.

S. R. May, R. F. Butler, and F. A. Roth, Magnetic polarity stratigraphy and stratigraphic completeness, *Geophys. Res. Lett.*, v. 12, 341–344, 1985.

I. McDougall, The present status of the geomagnetic polarity time scale, In: *The Earth: Its Origin, Structure and Evolution*, ed. M. W. McElhinny, Academic Press, London, pp. 543–566, 1979.

I. McDougall and F. H. Chamalaun, Geomagnetic polarity scale of time, *Nature*, v. 212, 1415–1418, 1966.

I. McDougall and D. H. Tarling, Dating of polarity zones in the Hawaiian Islands, *Nature*, v. 200, 54–56, 1963.

M. W. McElhinny, *Palaeomagnetism and Plate Tectonics*, Cambridge University Press, London, 356 pp., 1973.

P. L. McFadden and R. T. Merrill, Geodynamo energy source constraints from palaeomagnetic data, *Phys. Earth Planet. Inter.*, v. 43, 22–33, 1986.

L. W. Morley and A. Larochelle, Palaeomagnetism as a means of dating geological events, In: *Geochronology in Canada*, ed. F. F. Osborne, Roy. Soc. Canada Spec. Publ. No. 8, University of Toronto Press, Toronto, pp. 39–51, 1964.

T. Nagata, S. Uyeda, and S. Akimoto, Self-reversal of thermoremanent magnetism of igneous rocks, *J. Geomagnet. Geoelect.*, v. 4, 22–38, 1952.

G. Ness, S. Levi, and R. Couch, Marine magnetic anomaly timescales for the Cenozoic and Late Cretaceous: A precis, critique and synthesis, *Rev. Geophys. Space Phys.*, v. 18, 753–770, 1980.

N. D. Opdyke, Paleomagnetism of deep-sea cores, *Rev. Geophys. Space Phys.*, v. 10, 213–249, 1972.

N. D. Opdyke, L. H. Burckle, and A. Todd, The extension of the magnetic time scale in sediments of the central Pacific Ocean, *Earth Planet. Sci. Lett.*, v. 22, 300–306, 1974.

P. M. Sadler, Sediment accumulation rates and the completeness of stratigraphic sections, *J. Geology*, v. 89, 569–584, 1981.

L. Tauxe and N. D. Opdyke, A time framework based on magnetostratigraphy for the Siwalik sediments of the Khaur area, northern Pakistan, *Paleogeogr. Paleoclimat. Paleoecol.*, v. 37, 43–61, 1982.

L. Tauxe, D. V. Kent, and N. D. Opdyke, Magnetic components contributing to the NRM of Middle Siwalik red beds, *Earth Planet. Sci. Lett.*, v. 47, 279–284, 1980.

F. Theyer and S. R. Hammond, Palaeomagnetic polarity sequence and radiolarian zones, Brunhes to polarity epoch 20, *Earth Planet. Sci. Lett.*, v. 22, 307–319, 1974.

R. Thompson and F. Oldfield, *Environmental Magnetism,* Allen and Unwin, London, 1986, 227 pp.

F. J. Vine and D. H. Matthews, Magnetic anomalies over ocean ridges, *Nature*, v. 199, 947–949, 1963.